Influence of Optical Fluence Distribution on Photoacoustic Imaging

Mohamed K. Metwally, Sherif H. El-Gohary, Kyung Min Byun, Seung Moo Han, SooYeol Lee, Min Hyoung Cho, GonKhang, Jinsung Cho,Tae-Seong Kim

***Abstract*—**Photoacoustic imaging (PAI) is a non-invasive and non-ionizing imaging modality that combines the absorption contrast of light with ultrasound resolution. Laser is used to deposit optical energy into a target (i.e., optical fluence). Consequently, the target temperature rises, and then thermal expansion occurs that leads to generating a PA signal. In general, most image reconstruction algorithms for PAI assume uniform fluence within an imaging object. However, it is known that optical fluence distribution within the object is non-uniform. This could affect the reconstruction of PA images. In this study, we have investigated the influence of optical fluence distribution on PA back-propagation imaging using finite element method. The uniform fluence was simulated as a triangular waveform within the object of interest. The non-uniform fluence distribution was estimated by solving light propagation within a tissue model via Monte Carlo method. The results show that the PA signal in the case of non-uniform fluence is wider than the uniform case by 23%. The frequency spectrum of the PA signal due to the non-uniform fluence has missed some high frequency components in comparison to the uniform case. Consequently, the reconstructed image with the non-uniform fluence exhibits a strong smoothing effect.

***Keywords*—**Finite Element Method, Fluence Distribution, Monte Carlo Method, Photoacoustic Imaging.

I. Introduction

THE photoacoustic (PA) effect is a phenomenon where the electromagnetic (EM) energy is absorbed and converted into acoustic wave via thermoelastic expansion which generates ultrasound [1]. Photoacoustic imaging (PAI) in the medical field can combine the benefits of optical and ultrasound imaging. Optical imaging offers high contrast that can be achieved among biological tissues due to the differences of their optical absorptions. However, the optical imaging suffers from low penetration within biological tissues due to its high scattering. On the other hand, ultrasound imaging can achieve deep imaging with high resolution (45-720μm) due to its lowscattering and the wide frequency spectrum that is generated by the absorbing tissues [2].

The conversion of the EM energy into the PA signal in biological tissue involves multiple processes that include light propagation and absorption, temperature changes within the tissue, and thermal expansion of the tissue, and finally the generation of PA signals. To understand these complex processes, several analytical and numerical methods have been developed. By using these tools, researchers could get a better insight about the influence of various properties and parameters of PAI. For example, Rong et al. used finite element method (FEM) to study the effect of tissue elasticity on the received PA signal and showed that PAI has a potential to differentiate between the malignant and benign tumors based on their differential elasticity [3]. The effect of the object size was studied by FEM [4], producing some consistent results with the analytical findings of Li et al. [1]. On the other hand, the numerical methods have been used to optimize the design of PAI. Zhaohui et al. proposed a concave mirror utilized in the PAI system for deeper imaging based on their FEM findings [5]. All of these examples demonstrate the importance of using the numerical methods to improve the knowledge and design of PAI.

In general, the most common assumption in the previous studies is a uniform fluence (i.e., the deposited EM energy) within an imaging object [1], [6], [7]. This assumption is commonly considered in the forward solutions of PAI (i.e., PA wave generation and propagation) as well as solving the inverse problem (i.e., PA image reconstruction) [1]. This assumption could be accepted if the object is small enough to ensure uniform fluence. This small size can be defined based on the thermal diffusivity of the object and laser pulse duration [6]. However, the fluence distribution inside a larger object is not uniform as shown in many numerical studies [8], [9], it is expected that the assumption of uniform fluence distribution will not be accurate in the case of back-propagation imaging using a linear transducer.

In this work, we have investigated the influence of fluence distribution on the received PA signal with a linear transducer in the back-propagation imaging. We have simulated the light propagation by a Monte Carlo simulator and the PA process via FEM. Our results show that there is a significant smoothing effect of the non-uniform fluence in comparison to the uniform one.

This research was supported by the MSIP (Ministry of Science, ICT&Future Planning), Korea, under the ITRC (Information Technology Research Center) support program supervised by the NIPA(National IT Industry Promotion Agency) (NIPA-2014-(H0301-14-1003).

This work was supported by the Global Frontier R&D Program on <Human-centered Interaction for Coexistence> funded by the National Research Foundation of Korea grant funded by the Korean Government (MSIP)(2012M3A6A3056426).

Mohamed K. Metwally, Sherif H. El-Gohary, Kyung Min Byun,Seung Moo Han,SooYeol Lee, Min Hyoung Cho, GonKhang, and Tae-Seong Kim are with the Department of Biomedical Engineering, Kyung Hee University, Yongin, Gyeonggi, Republic of Korea. (phone: +82-31-201-3731; fax: +82-31-201-3666; e-mail: tskim@ khu.ac.kr).

Jinsung Cho is with Department of Computer Engineering, Kyung Hee University, Yongin, Gyeonggi, Republicof Korea (e-mail: chojs@khu.ac.kr).

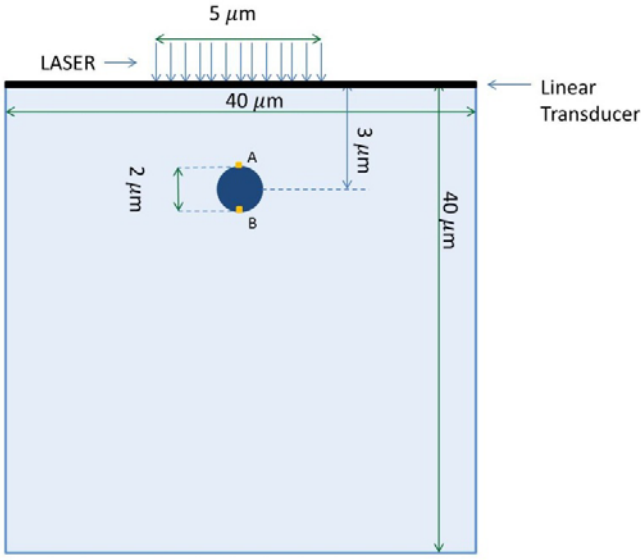

Fig.1 A schematic diagram of 2-D cross-section of the 3D tissue model

II. Methods

A. The Tissue Model

A simple 3-D model of breast with cancer was simulated where the breast was modeled as a cylinder of 40 μm height and 20 μm radius encompasses a tumor that was modeled as a sphere of 1 μm radius. The depth of the tumor was 3 μm beneath the surface of the breast as shown in Fig. 1. The laser source in our simulation covers a rectangular surface area of 5x5 μm^2 of the homogeneous breast. This 3-D model was used to solve for light propagation via Monte Carlo method.

Although the PA phenomenon is actually of a 3-D nature, where each point on the surface of the PA source participates in the final PA signal in the back-propagation imaging, a linear transducer with anisotropic detection response is practically used to reconstruct a 2-D PA image [10]. In fact, any signal from out-of-plane sources will be relatively rejected, while the detector will give high response to the signal that is coming from the perpendicular plane to the transducer. Therefore a 2-D model was used to simulate the thermal and acoustical propagation in this study. Note that the physical dimensions were minimized for reasonable computation time.

B. PA Simulation

1. Light Propagation

As the first step, to understand how light propagates through the tissues; Monte Carlo method was used to compute the photon transport in a turbid medium such as tissues in which absorption and scattering occur.

Monte Carlo simulation aims at solving a random walk process, where a photon or a photon package is traced through the tissue until it exits or gets entirely absorbed. By repeating this process for a large number of photon packages, it is possible to obtain statistics for these physical quantities. Boundary conditions are determined by means of Snell's law at the tissue-air interface. The procedure describing the simulation is reported in detail elsewhere [11].

As a result for the random walk process, the photons will not be absorbed equally within the tumor. Therefore, some regions within the tumor will absorb more photons than others at different times as will be shown later.

In our Monte Carlo simulation, we used a set of 10^6 randomized photons. The optical properties of the breast and tumor tissues are presented in Table I [8]. The simulations were performed at the wavelengths of 1064 nm to provide discrimination between the tumor and surrounding breast tissues within the model.

TABLE I
Optical Properties for the Breast and Tumor Tissues Used in the Model

Tissue	Absorption Coefficient (mm^{-1})	Scattering Coefficient (mm^{-1})	Anisotropy	Refractive Index
Breast	0.02	16.7	0.9	1.4
Tumor	0.74	9	0.9	1.4

2. Heat Distribution

The temperature in the tumor changes as a result to the photons absorption. This change in temperature distribution can be described by the following bio-heat equation:

$$\rho C \frac{\partial T}{\partial t} - \nabla.(K \nabla T) = H \ , H = \varnothing \mu \qquad (1)$$

where ρ is the density, C the specific heat capacity, *k* the thermal conductivity, *T* the temperature. *H* is the heat generation rate (e.g., the heat source in W/m^3), which is a result of multiplication of μ, the optical absorption coefficient (in m^{-1}), to Ø, the fluence rate (in J/m^2). The blood perfusion effect is ignored because the laser shining time is less than the thermal confinement time [1], [7]. Table II shows the assigned values of the thermal properties of the tumor and normal breast tissues [8].

TABLE II
Thermal Properties for the Breast and Tumor Tissues in the Model

Tissue	Density (kg/m^3)	Specific Heat Capacity (J/kg.k)	Thermal Conductivity (W/m.k)
Breast	998	840	0.7
Tumor	1000	4181.3	1.1

3. Thermal Expansion

As a result to the temperature changes within the tumor, the tumor undergoes thrmoelastic expansion while the temperature rises and shrinking when the temperature drops. This process can be described by the displacement equation [3]:

$$\rho \frac{\partial^2 u}{\partial t^2} - \frac{E}{2(1+\sigma)(1-2\sigma)} \nabla(\nabla.u) - \frac{E}{2(1+\sigma)} \nabla^2 u = \frac{-\beta E}{3(1-2\sigma)} \nabla T \qquad (2)$$

where *u* is the displacement in (m), *E* the Young's modulus, σ

the Poisson's ratio, and β the thermal expansion. Table III shows the mechanical properties of the normal breast and tumor tissues [3], [8].

TABLE III
MECHANICAL PROPERTIES OF THE BREAST AND TUMOR TISSUES IN THE MODEL

Tissue	Young's Modulus (Kpa)	Poisson Ratio	Thermal Expansion (K^{-1})
Breast	27	0.495	1.4×10^{-5}
Tumor	270	0.495	8.5×10^{-6}

4. PA Signal Generation

The acceleration in the tumor displacement is converted into initial pressure (p) based on the following conversion equation [12]:

$$\frac{\partial p}{\partial n} = -\rho \frac{\partial^2 u_n}{\partial t^2} \tag{3}$$

where u_n is the displacement in the direction of the wave propagation. The initial wave propagates through the normal breast tissue medium based on the homogeneous wave equation:

$$\nabla p(r,t) = \frac{1}{v_s^2}\frac{\partial^2 p(r,t)}{\partial t^2} \tag{4}$$

The sound speed, v_s within the normal breast and tumor tissues are assigned as 1450 m/s and 1540 m/s respectively [8].

The numerical simulation was done by ANSYS [13] and the sparse solver was used to calculate the displacement and the propagating PA pressure waves. The FE model included 67,757 nodes and 67,363 elements with the element quality in a range from 0.5 to 0.86.

C. Fluence Settings

In order to investigate the effect of fluence uniformity on the PA signal, two fluence distributions were considered: 1) uniform and 2) non-uniform fluence within the tumor. The uniform fluence was simulated by applying one fluence value at a time to all points within the tumor. The uniform fluence waveform over time followed a triangular distribution with a central time of 2.65 ns with the full-width half-maximum (FWHM) value of 1.25 ns and the maximum fluence value of 371.4 W/m^2. The non-uniform fluence was resulted from the Monte Carlo simulation of light propagation within the model due to the laser shining for 2.5 ns. It was considered that the total deposited energy within the tumor in the case of uniform fluence to be equivalent to the total deposited energy in the case of non-uniform fluence which is 0.511×10-4 mJ/cm^2 in this study.

D. Analytical Method

In order to validate the PA simulation, the received PA signal due to the uniform fluence case was compared to the analytical solution for the PA signal generation [14]. The analytical equation that describes the received PA signal at distance r is:

$$p(r,t) = \frac{\beta E H(t-\tau)}{2(2\pi)^{3/2} r C_p \tau_e^3}\exp(-0.5(\frac{t-\tau}{\tau_e})^2)\ ; \quad \tau = \frac{r}{v}\ ;\ \tau_e \approx \frac{R_s}{v} \tag{5}$$

where β is the thermal expansion of the source, E Young's modulus, C_p the specific heat capacity, and v the sound speed. The source was considered as a circle with a radius of R_s = 1 μm and the signal was calculated at distance r = 3 μm. The waveform of the fluence rate was the same applied waveform in the uniform fluence case.

III. RESULTS

A. The PA Signal Validation

To validate the numerical procedure, we have computed a PA signal using an analytical equation in [14] and compared to our numerically derived PA signal with uniform fluence distribution. Fig. 2 shows both of the PA signals of the analytical equation and the numerical simulation. The correlation between both signals was about 90%.

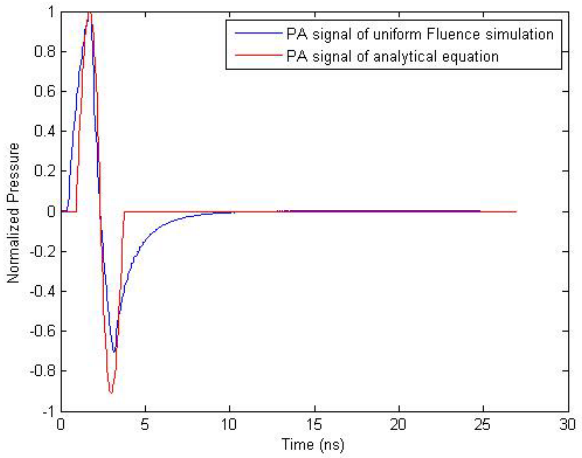

Fig. 2 The analytical PA signal (in red) versus the numerical PA signal (in blue)

B. Influence of Fluence Distribution

Fig. 3 shows the of the normalized uniform and non-uniform fluence 2-D distributions within the tumor at different time instants. It is expected that the change in the distribution will affect the generation and propagation of the PA wave. Fig. 4 shows the generation of the PA wave in both cases. It isobserved that there is asymmetry in the generation of PA wave with the non-uniform fluence where the signal generated first from the tumor side that confronts the laser, is stronger than the opposite side of the tumor.

Fig. 5 shows the received PA signals by the middle element of the transducer at the distance of 3 μm from the center of the tumor in the cases of the uniform and non-uniform fluence and their frequency spectrum. The results show that the non-uniform fluence deforms the generated PA signal: the signal is not a smooth N-like wave as that of the uniform fluence case.

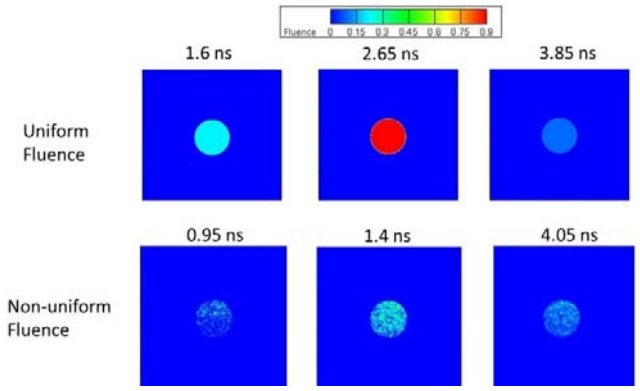

Fig.3 2D distributions of the normalized uniform (the upper row) and non-uniform (the lower row) fluence distributions within the tumor at different time instants

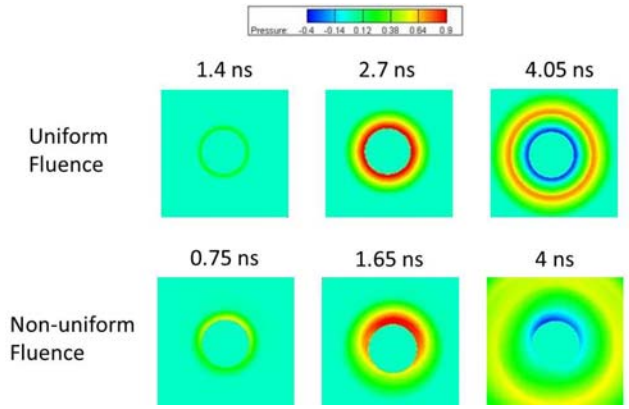

Fig. 4 Screen shots of the propagating PA waves in the case of uniform (the upper row) and non-uniform (the lower row) Fluence

It is observed that the non-uniform fluence broadens the PA signal which is clearly shown in the frequency spectrum. Note that the frequency spectrum of the PA signal in the case of non-uniform fluence is missing some high frequency components with respect to the frequency spectrum of the PA signal in the case of uniform fluence. Fig. 6 shows the reconstructed images using the FFT reconstruction algorithm [15]. Quantitatively, the full-width half-maximum (FWHM) of the PA signal was calculated for the PA signal of both cases. Table IV shows that the non-uniform fluence broadens the PA signal about 23% more than the PA signal in the case of the uniform fluence. The size of the reconstructed object was determined by calculating the FWHM of the horizontal intensity profile at 3μm under the transducer. Note that the FWHM of the intensity profile in the case of the non-uniform fluence is wider than the FWHM in the case of uniform fluence by 45%.

IV. Discussion

This study aimed at investigating the influence of the fluence distribution on the PA back-propagation imaging. The investigation was done using Monte Carlo method to estimate the light propagation and fluence distribution within the model and FEM to simulate the PA wave generation.

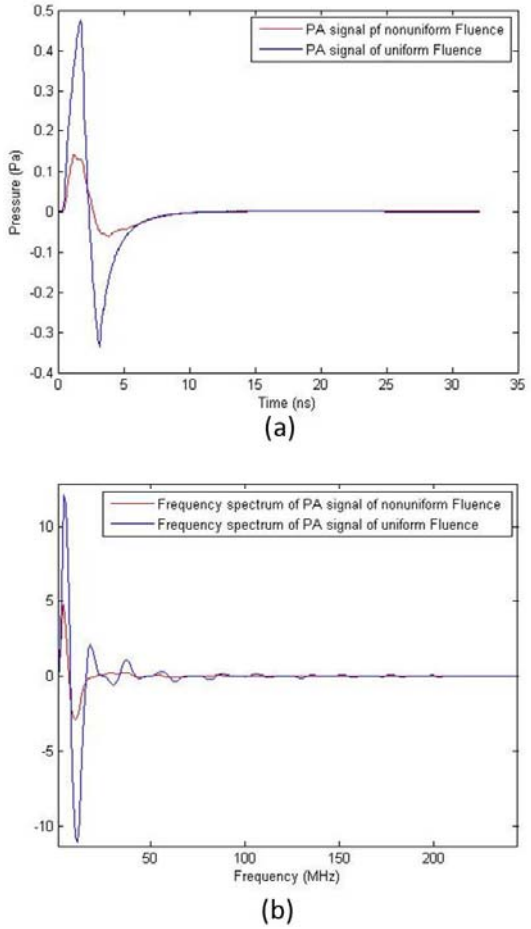

Fig.5 PA signals and their spectra. (a) The received PA signals by the middle transducer element, (b) the frequency spectrum of the PA signals in the cases of uniform and non-uniform Fluence

TABLE IV
Quantitative Analysis of the Generated PA Signal in the Case of Uniform And Non-Uniform Fluence

	Maximum PA Pressure (Pa)	FWHM of PA Signal (ns)	FWHM of Image (μm)
Uniform Fluence Case	0.47	1.15	2.31
Non-uniform Fluence Case	0.14	1.41	3.35

The simulation results demonstrate that the non-uniform fluence tends to broaden the PA signal more than the case of the uniform fluence. This phenomenon can be explained by the photons trajectories. When the laser is applied, some photons can reach directly to the target and absorbed there, however many other photons may follow other longer trajectories due to the scattering within the media. Therefore, the object will not absorb the energy within the same time period of laser exposure, but it will take longer time. Consequently, the temperature will change in a slower rate than the uniform fluence case, which will broaden the PA signal and reduce its amplitude. As a result, the frequency spectrum will lose some high frequency components which will result in a smoothing effect in the reconstructed image. This phenomenon should be considered in the reconstruction

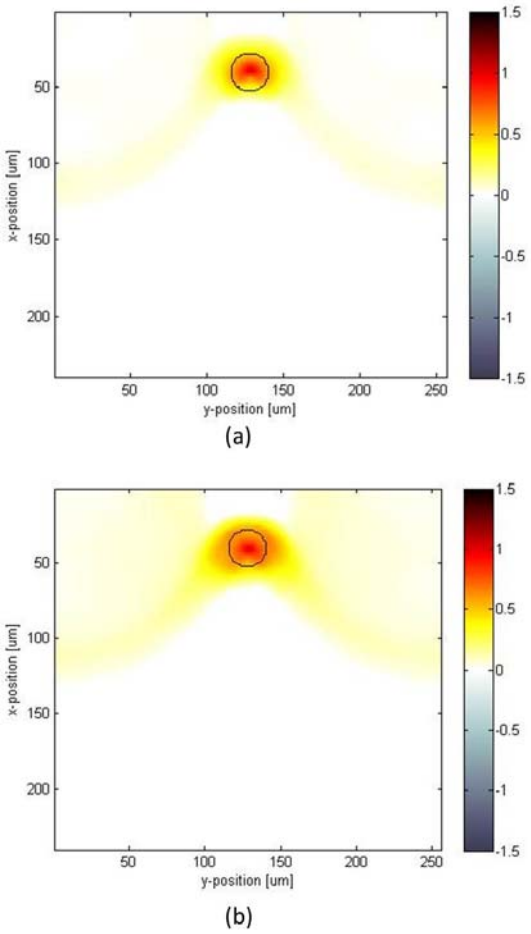

Fig. 6 Reconstructed PA images in the case of (a) uniform and (b) non-uniform fluence. The black circle shows the true boundaries of the simulated tumor

algorithms of PAI because it affects the accuracy of PA back-propagation imaging.

V. Conclusion

The results of this study show that the non-uniform fluence affects significantly the PA back-propagation imaging by broadening the PA signals and smoothing PA images. This suggests that the non-uniform fluence distribution should be taken into account in PAI.

References

[1] C. Li, and L. V. Wang, "Photoacoustic tomography and sensing in biomedicine," *Phys. Med. Biol*., vol. 54, no. 19, pp. R59- R97, 2009.

[2] L. V. Wang, and S. Hu, "Photoacoustic tomography: in vivo imaging from organelles to organs," *Science*, vol. 335, no. 6075, pp. 1458-1462, 2012.

[3] R. R. An, X. S. Luo, and Z. H. Shen, "Numerical simulation of the influence of the elastic modulus of a tumor on laser-induced ultrasonics in soft tissue," *Applied Optics*, vol. 51, no. 32, pp. 7869- 7876, 2012.

[4] R. An, X. Luo, and Z. Shen, "Numerical and experimental investigation of the influence of tumor size on laser-induced ultrasonics in soft tissue," *Laser Physics*, vol. 24, no. 4, 2014.

[5] Z. Wang, S. Ha, and K. Kim, "Photoacoustic design parameter optimization for deep tissue imaging by numerical simulation," *Photons Plus Ultrasound: Imaging and Sensing Proc. SPIE* , vol. 8223, pp. 822346-1-8, 2012.

[6] Y.-L. Sheu, and P.-C. Li, "Simulation of photoacoustic wave propagation using a finite-difference time-domain method with Berenger's perfectly matched layers," *J. Acoust. Soc. Am*., vol. 124, no. 6, pp. 3471-3480, 2008.

[7] S. Telenkov, A. Mandelis, B. Lashkari, and M. Forcht, "Frequency-domain photothermoacoustics: alternative imaging modality of biological tissues," *J. Appl. Phys*., vol. 105, issue 10, pp. 102029-1-8, 2009.

[8] Z. Wang, S. Ha, and K. Kim, "Evaluation of finite element based simulation model of photoacoustics in biological tissues,"*Proc. SPIE, Medical Imaging: Ultrasonic Imaging, Tomography, and Therapy*, vol. 8320, pp. 83201L1-9, 2012.

[9] B. Banerjee, S. Bagchi, R. M. Vasu, and D. Roy, "Quantitative photoacoustic tomography from boundary pressure measurements: noniterative recovery of optical absorption coefficient from the reconstructed absorbed energy map," *J. Opt. Soc. Am. A*., vol. 25, no. 9, pp. 2347-2356, 2008.

[10] K. P. Köstli, and P. C. Beard, "Two-dimensional photoacoustic imaging by use of Fourier-transform image reconstruction and a detector with an anisotropic response," *Applied Optics*, vol. 42, no. 10, pp. 1899-908, 2003.

[11] L. H. Wang, S. L. Jacques, and L. Zheng , "MCML-Monte-Carlo modeling of light transport in multilayered tissues," *Computer Methods and Programs in Biomedicine*, vol. 47, pp. 131-146, 1995.

[12] M. K. Metwally, H.-S. Han, H. J. Jeon, G. Khang, and T.-S. Kim, " Influence of the anisotropic mechanical properties of the skull in low-intensity focused ultrasound towards neuromodulation of the brain," *in Proc. 35th Annu. Inter. Conf. of IEEE EMBC*, pp. 4565-4568, 2013.

[13] ANSYS available: http://www.ansys.com

[14] C. G. A. Hoelen and F. F. M. de Mul, "A new theoretical approach to photoacoustic signal generation," *J. of Acoust. Soc. Am*., vol. 106, no. 2, pp. 695-705, 1999.

[15] J. I. Sperl, K. Zell, P. Menzenbach, C. Haisch, S. Ketzer, M. Marquart, H. Koenig, and M. W. Vogel, " Photoacoustic image reconstruction -A quantitative analysis," *Novel Optical Instrumentation for Biomedical Applications III. SPIE*, vol. 6631, pp. 663103-1-12, 2007.